Global Biogeochemical Cycles

RESEARCH ARTICLE
10.1029/2019GB006242

Dinitrogen Fixation Across Physico-Chemical Gradients of the Eastern Tropical North Pacific Oxygen Deficient Zone

C. R. Selden[1], M. R. Mulholland[1], P. W. Bernhardt[1], B. Widner[1,2], A. Macías-Tapia[3,1], Q. Ji[4,5], and A. Jayakumar[3]

[1]Department of Ocean, Earth & Atmospheric Science, Old Dominion University, Norfolk, VA, USA, [2]Now at Department of Marine Chemistry and Geochemistry, Woods Hole Oceanographic Institution, Woods Hole, MA, USA, [3]Institute of Oceanological Research, Autonomous University of Baja California, Ensenada, Mexico, [4]Department of Geosciences, Princeton University, Princeton, NJ, USA, [5]Now at Helmholtz Center for Ocean Research Kiel, Kiel, Germany

Key Points:
- Dark, oxygen-deplete waters in the region harbor N_2 fixers, but their activity is patchy and limited by organic carbon
- N_2 fixation rates were high in inshore euphotic waters, suggesting that coastal zones harbor more N_2 fixation than previously thought
- N_2 fixation occurs in the region, but rates appear too low to compensate for reactive N losses on a local scale

Supporting Information:
- Supporting Information S1
- Table S1

Correspondence to:
C. R. Selden,
cseld001@odu.edu

Citation:
Selden, C. R., Mulholland, M. R., Bernhardt, P. W., Widner, B., Macías-Tapia, A., Ji, Q., & Jayakumar, A. (2019). Dinitrogen fixation across physico-chemical gradients of the Eastern Tropical North Pacific oxygen deficient zone. *Global Biogeochemical Cycles*, *33*, 1187–1202. https://doi.org/10.1029/2019GB006242

Received 5 APR 2019
Accepted 2 SEP 2019
Accepted article online 4 SEP 2019
Published online 13 SEP 2019

Abstract The Eastern Tropical North Pacific Ocean hosts one of the world's largest oceanic oxygen deficient zones (ODZs). Hot spots for reactive nitrogen (N_r) removal processes, ODZs generate conditions proposed to promote N_r inputs via dinitrogen (N_2) fixation. In this study, we quantified N_2 fixation rates by ^{15}N tracer bioassay across oxygen, nutrient, and light gradients within and adjacent to the ODZ. Within subeuphotic oxygen-deplete waters, N_2 fixation was largely undetectable; however, addition of dissolved organic carbon stimulated N_2 fixation in suboxic (<20 μmol/kg O_2) waters, suggesting that diazotroph communities are likely energy limited or carbon limited and able to fix N_2 despite high ambient concentrations of dissolved inorganic nitrogen. Elevated rates (>9 nmol $N{\cdot}L^{-1}{\cdot}day^{-1}$) were also observed in suboxic waters near volcanic islands where N_2 fixation was quantifiable to 3,000 m. Within the overlying euphotic waters, N_2 fixation rates were highest near the continent, exceeding 500 μmol $N{\cdot}m^{-2}{\cdot}day^{-1}$ at one third of inshore stations. These findings support the expansion of the known range of diazotrophs to deep, cold, and dissolved inorganic nitrogen-replete waters. Additionally, this work bolsters calls for the reconsideration of ocean margins as important sources of N_r. Despite high rates at some inshore stations, regional N_2 fixation appears insufficient to compensate for N_r loss locally as observed previously in the Eastern Tropical South Pacific ODZ.

Plain Language Summary Nitrogen is an essential component of life's building blocks. Lack of nitrogen can limit growth of phytoplankton, the photosynthetic microbes at the base of most oceanic food webs. Phytoplankton in the surface ocean facilitate the removal of carbon dioxide, a strong greenhouse gas, from the atmosphere by converting it to organic forms that can aggregate and sink. Therefore, understanding the factors that control the ocean's nitrogen reservoir is important to predicting Earth's future climate. Previous research has suggested that nitrogen inputs and losses may occur in close spatial proximity because nitrogen loss processes result in a nitrogen deficit, which is thought to favor dinitrogen (N_2) fixation—the microbe-mediated conversion of unreactive N_2 gas to a bioavailable form. Here, we measured rates of N_2 fixation in an important region of nitrogen loss. We found that rates of N_2 fixation in the region were low, suggesting that nitrogen input and removal processes do not occur in close spatial proximity here. Nevertheless, high rates of N_2 fixation were observed near shore and volcanic islands, suggesting that N_2 fixation can occur here but was restricted. This study contributes to our understanding of N_2 fixation in a globally important region likely to change as Earth warms.

1. Introduction

One of the major sources of reactive N (N_r) to the global ocean is dinitrogen (N_2) fixation (Gruber & Galloway, 2008), the assimilation of N_2 gas into biomass. Despite the abundance of N_2 in marine systems, only selected prokaryotic "N_2 fixers" (diazotrophs) have the genetic capacity to mediate its intracellular reduction to ammonia, which can then be assimilated via common metabolic pathways (Berges & Mulholland, 2008). Where present, these organisms can increase the N_r pool and consequently stimulate primary production in N-limited ocean regions, thereby enhancing atmospheric drawdown of carbon dioxide (CO_2) and, potentially, export of this carbon (C) through the biological pump (e.g., Karl et al., 2012). Understanding the factors regulating N_r inputs and losses is essential to predicting

how oceanic N_r inventories vary under changing climatic conditions and affect the ocean's capacity to take up CO_2.

Historically, N_2 fixation has been ascribed primarily to filamentous cyanobacteria that thrive in nutrient-deplete tropical and subtropical waters where warm temperatures and low dissolved inorganic N (DIN) concentrations are thought to promote diazotrophy (Carpenter & Capone, 2008; Flores & Herrero, 2005; Mulholland et al., 2001). Recent work has challenged this paradigm, expanding the range of N_2 fixation to include cooler (Blais et al., 2012; Harding et al., 2018; Moisander et al., 2010; Sipler et al., 2017), aphotic (Benavides et al., 2015, 2016; Bonnet et al., 2013; Rahav et al., 2013, 2015), and mesotrophic (Knapp, 2012; see also Bentzon-Tilia et al., 2015; Bonnet et al., 2013; Farnelid et al., 2013; Grosse et al., 2010; Mulholland et al., 2012; Rees et al., 2009; Sohm et al., 2011) waters. Concomitantly, appreciation has grown for the importance of diverse and broadly distributed diazotrophic clades, including eukaryote symbionts (e.g., Martinez-Perez et al., 2016; Moisander et al., 2010) and noncyanobacterial diazotrophs (Bombar et al., 2016; Moisander et al., 2017, and references therein), to the global N cycle. The sensitivities and physiological ranges of these groups likely differ from those of long-cultured and well-studied cyanobacterial diazotrophs like *Trichodesmium*, complicating our understanding of the environmental factors that regulate the magnitude and distribution of N_2 fixation rates (NFR) in the ocean.

Based on early studies of freshwater and tropical cyanobacterial diazotrophs, it was determined that significant concentrations (i.e., $\geq$1 μM) of ambient DIN should preclude N_2 fixation, an energetically costly means of acquiring N (Falkowski, 1983; Knapp, 2012); yet, recent work suggest that this paradigm must be revisited (Knapp, 2012; see also Bentzon-Tilia et al., 2015; Bonnet et al., 2013; Farnelid et al., 2013; Grosse et al., 2010; Mulholland et al., 2012, 2019; Rees et al., 2009; Sohm et al., 2011). There are a variety of reasons organisms may fix N_2 despite its energetic costs. Certain organisms, including some eukaryote symbionts, lack the genetic ability to reduce nitrate (NO_3^-; Caputo et al., 2018); investing in NO_3^- assimilation machinery may be unfavorable for diazotrophs already growing on N_2 (Karl et al., 2002), and some diazotrophs may use N_2 fixation as a mechanism for regulating intracellular state (Bombar et al., 2016), potentially decoupling its activity from N demand satiety. One energetic complication is that nitrogenase, the enzyme that mediates N_2 fixation, is permanently inhibited by O_2 (Postgate, 1998), and oxygenic diazotrophs as well as those inhabiting oxic environments must invest in O_2 avoidance strategies to minimize nitrogenase turnover (Vitousek et al., 2002). Diazotrophs in anoxic environments could evade this cost, potentially making N_2 fixation more favorable (Großkopf & LaRoche, 2012). Active N_2 fixation has now been observed in low-O_2 waters despite ambient DIN concentrations in excess of 1 μM (Bonnet et al., 2013; Dekaezemacker et al., 2013; Farnelid et al., 2013; Fernandez et al., 2011; Hamersley et al., 2011; Jayakumar et al., 2017; Loescher et al., 2014), as well as in ammonium (NH_4^+)-rich anoxic sediments (e.g., Andersson et al., 2014; McGlathery et al., 1998).

There are three major O_2-deplete regions of the pelagic ocean—in the Eastern Tropical North Pacific (ETNP), Eastern Tropical South Pacific (ETSP), and Arabian Sea (DeVries et al., 2012). The O_2 minimum zones (OMZs), that is, the low-O_2 depth horizon, and O_2 deficient zones (ODZs), where O_2 is undetectable using common sensors, are predominantly below the euphotic zone (Paulmier & Ruiz-Pino, 2008). The majority of N_2 fixation within such waters is consequently mediated by noncyanobacterial diazotrophs (Chang et al., 2019; Jayakumar et al., 2012, 2017), some portion of which are presumably heterotrophic. Heterotrophic diazotrophs can become organic C-limited, particularly in deep waters, and organic C availability may therefore constrain their NFR (Bombar et al., 2016). Indeed, dissolved organic C additions has enhanced NFR in both mesopelagic (Benavides et al., 2015; Bonnet et al., 2013; Rahav et al., 2013) and epipelagic waters (Loescher et al., 2014; Rahav et al., 2015).

Pelagic ODZs account for roughly one third of N_r loss from the ocean (DeVries et al., 2012). Significant N_r deficits are observed in these regions relative to the concentrations of other dissolved constituents including phosphate (soluble reactive phosphate, SRP) and iron (Fe), an essential cofactor in the nitrogenase enzyme (Dixon & Kahn, 2004). As such, these waters are hypothesized to favor diazotrophic activity once advected into the euphotic zone, where the remaining DIN is rapidly depleted, by limiting the growth of competitors who cannot fix N_2 (Deutsch et al., 2007; Monteiro et al., 2011). In so doing, these geochemical signals (e.g., low DIN:SRP) are believed to play a critical role in the feedback mechanism between N_2 fixation and N_r losses regulating the ocean's N_r inventory (Weber & Deutsch, 2014); however, Fe limitation of N_2 fixation

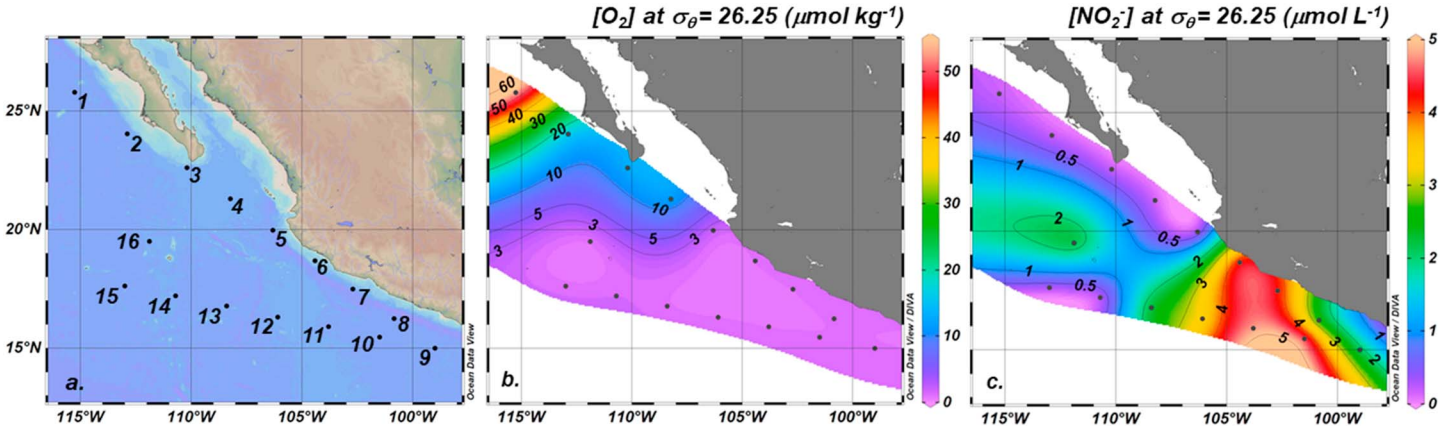

Figure 1. Bathymetry overlain by station numbers (a) and dissolved O_2 (μmol/kg) and nitrite (NO_2^-, μM) concentrations, collected using the Sea-Bird CTD and Pump Profiling System respectively, along an isopycnal surface $\sigma_\theta = 26.25$ (b, c), illustrating the extent of the study region and oxygen deficient zone. Oxygen deficiency was defined by O_2 concentrations below detection (3 μmol/kg) and NO_2^- concentrations exceeding 0.5 μM.

may spatially decouple N_r inputs from losses (Weber & Deutsch, 2014), as hypothesized for the South Pacific basin (Bonnet et al., 2017; Dekaezemacker et al., 2013; Knapp et al., 2016, 2018; Weber & Deutsch, 2014). The North Pacific receives higher aeolian Fe inputs than the South Pacific Ocean (Jickells et al., 2005), but N_2 fixation measurements in the ETNP ODZ region remain sparse despite local observations of diazotrophs (Jayakumar et al., 2017; White et al., 2013).

This study leveraged naturally occurring light, nutrient, and O_2 gradients in the ETNP to characterize N_2 fixation by mixed diazotroph communities with respect to these variables. The influence of dissolved organic C availability on N_2 fixation below the euphotic zone was investigated by amending whole water incubations with either glucose or a mixed amino acid solution. By furthering understanding of the physico-chemical factors regulating diazotroph activity, this study contributes to our evolving view of N_2 fixation in the marine environment and the feedback mechanisms maintaining the ocean's N_r inventory.

2. Materials and Methods

We measured NFR, nutrient concentrations, and hydrographic characteristics within and adjacent to the ETNP ODZ aboard the National Oceanic and Atmospheric Administration vessel *Ronald H. Brown* in April 2016, during an El Niño–Southern Oscillation (ENSO) event (Climate Prediction Center, 2019). The cruise track extended southeast along the Mexican coastline from the Rosa Seamount (25°N, 115°W) off the Baja peninsula to 15°N and 99°W, proximal to the Guerrero-Oaxaca border, then offshore in a northwesterly direction to 18°N and 113°W (Figure 1a). "Inshore" was defined here as being within 200 km of the coastline; however, all stations were beyond the shelf break and were at least 2,000 m deep. Our sampling strategy was optimized for high-resolution data collection along vertical gradients of light, dissolved nutrients, and O_2.

2.1. Hydrographic and Nutrient Measurements

Vertical profiles of temperature, salinity, O_2, and chlorophyll *a* fluorescence were obtained at 16 stations using a Sea-Bird SBE 11plus CTD, equipped with a model 43 dissolved oxygen sensor (detection limit ~3 μmol/kg O_2), a LI-COR Biospherical Photosynthetically Available Radiation (PAR) Sensor, and a Seapoint Chlorophyll Fluorometer. These instruments were mounted to a sampling rosette holding twenty-four 12-L Niskin bottles from which water samples were collected at selected depths to measure chlorophyll *a* and dissolved nutrient concentrations. Water for N_2 fixation incubations in the euphotic zone and below the ODZ was also collected from Niskin bottles (see below). Chlorophyll *a* concentrations were determined via the nonacidification method (Welschmeyer, 1994). NO_3^- plus nitrite (NO_2^-) and SRP concentrations were measured onboard using an Astoria-Pacific nutrient autoanalyzer following standard colorimetric methods (Parsons et al., 1984) and according to the manufacturer's specifications. A Biosciences Ultrospec 2100 *pro* spectrophotometer was used for NO_2^- analysis (Parsons et al., 1984), and NO_3^- concentrations were calculated by difference. NH_4^+ concentrations were determined fluorometrically using the

Table 1
Summary of N_2 Fixation Rate Measurement Incubation Protocols Above (EUPH), Within (OMZ), and Below (DEEP) the Oxygen Minimum Layer (Typically ~150–400 m)

Depth horizon	Bottle type	Collection protocol	Incubation conditions	Duration
EUPH	Clear PETG bottles (1 L)	Collected in shaded 10-L carboys from Niskin bottles	Incubated in appropriately shaded on-deck tanks with continuously flowing surface seawater	~24 hr
OMZ	Amber glass bottles (4 L)	Collected anoxically and directly from depth using pump	Incubated in the dark in a walk-in cold van at ~12 °C	~24 hr
DEEP	Amber glass bottles (4 L)	Collected in shaded 10-L carboys from Niskin bottles	Incubated in the dark in either ~12 °C cold van or 4 °C walk-in refrigerator	~48 hr

Note. Note that not all "OMZ" samples exhibit suboxia (<20 μmol/kg). See Text S1 for a detailed description of sample handling. OMZ = O_2 minimum zone.

orthophthaldialdehyde method (Holmes et al., 1999). DIN was calculated as the sum of NO_3^-+NO_2^- and NH_4^+ concentration. Further details of these analyses are available in the supporting information Text S1.

In addition to discrete measurements, a Pump Profiling System, developed and built by the Monterey Bay Aquarium and Research Institute (Sakamoto et al., 1990), was used to generate near-continuous nutrient profiles in real time to approximately 350 m and to collect low-oxygen water. This system was composed of a cable, hose, and a small rosette to which a submersible water pump, a Sea-Bird SBE 19 SeaCAT CTD, WETStar Fluorometer, Sea Tech Beam Transmissometer, and a LI-COR Biospherical PAR Sensor were mounted. The Pump Profiling System was deployed to a maximum depth of 400 m. Water was pumped directly from depth to the laboratory to generate in situ nutrient profiles and to an on-deck station where samples from the O_2 minimum depth horizon were collected for incubation experiments (see below). In the laboratory, this flow ran first through an MBARI-modified Durafet pH sensor before being shunted to an Alpkem Astoria-Pacific Rapid Flow Analysis System which determined concentrations of NO_3^- plus NO_2^-, NO_2^-, and NH_4^+ at a rate of one measurement per second. NO_3^- and NO_2^- measurements were made following manufacturer's instructions (Sakamoto et al., 1990). The orthophthaldialdehyde method (Holmes et al., 1999) was adapted for the Rapid Flow Analysis System and used to determine in situ NH_4^+ concentrations. A Fast Repetition Rate Fluorometer collected chlorophyll *a* fluorescence profiles at a rate of one sample per 30 s.

2.2. N_2 Fixation Incubation Experiments

Whole water was collected from the Niskin bottles or pumped from depth anoxically using the Pump Profiling System for N_2 fixation incubation experiments carried out above, below or within the OMZ, respectively (Table 1). We define the OMZ as the region of the water column in which the lowest O_2 concentrations were observed at a site. This is distinct from the ODZ, operationally defined by O_2 concentrations below the limit of detection (LOD) of the Seabird O_2 sensor (3 μmol/kg) and NO_2^- concentrations exceeding 0.5 μM which has been deemed indicative of functionally anoxic conditions (Thamdrup et al., 2012).

NFR measurements were made using a modified version of the traditional $^{15}N_2$ bubble method (Montoya et al., 1996). In the traditional $^{15}N_2$ bubble method, $^{15}N_2$ gas is injected into a filled sample bottle and ^{15}N enrichment of the particulate N (PN) pool is measured following an incubation period. The assimilation rate of the ^{15}N tracer into biomass (i.e., NFR) can then be calculated using a mixing model as shown below (equation (1); Montoya et al., 1996). N_2 gas is, however, slow to equilibrate, causing source pool enrichment (i.e., dissolved N_2 enrichment) to change over the course of the incubation which may result in an underestimation of NFR (Böttjer et al., 2017; Großkopf et al., 2012; Mohr et al., 2010). To address this issue, the dissolution of highly enriched $^{15}N_2$ gas (~99%, Cambridge Isotopes, Tewksbury, MA) was hastened following injection by slowly inverting sample bottles on a large seesaw for 15 min. The seesaw consisted of a flat panel affixed to a central axis with baskets on either side in which incubation bottles were secured laterally. In this configuration, the $^{15}N_2$ gas bubble traveled the full length of each bottle as the panel was gently rocked. Cambridge Isotope $^{15}N_2$ gas was selected because, while significant ^{15}N-NH_4^+ and -NO_3^- concentrations have been observed in other brand stocks, these contaminants have only been reported from Cambridge Isotope stocks at tracer-level concentrations (Dabundo et al., 2014). The remaining gas bubble was then

removed using a syringe prior to the incubation period, and ^{15}N enrichment of the N_2 pool was measured directly (see below). $^{15}N_2$ uptake experiments were carried out in triplicate. A detailed description of sample collection and incubation procedures is available in the supporting information Text S1.

Euphotic samples were incubated on-deck in tanks equipped with neutral density screens to approximate light levels at the depth of sample collection, which was determined using the PAR sensor mounted to the CTD rosette. Continuously flowing surface seawater maintained near-ambient surface temperatures in the deck incubators. Subeuphotic waters (below the 0.1% light level; Table 2) were incubated in the dark, in either a ~12 °C cold van or a 4 °C walk-in refrigerator, depending on the temperature at the depth of sample collection. Due to a cold van malfunction, incubations from within the OMZ at Stations 8, 9, and 10 were carried out in a darkened room retrofitted with air conditioners, capable of maintaining temperatures at ~16 °C. While warmer temperatures may increase metabolic activity (Price & Sowers, 2004), the effect of this slight increase in temperature on N_2 fixation was likely minimal as rates from the affected bottles were largely undetectable (Table S2). For samples above and within the OMZ or ODZ, uptake experiments were 24 hr. Water samples collected below the OMZ or ODZ, where biomass is lower and cooler temperatures reduce metabolic rates (Price & Sowers, 2004), were incubated for 48 hr. Incubations were terminated by filtration of the sample onto precombusted (450 °C for 2 hr) Whatman GF-75 filters (nominal pore size of 0.3 μm). Immediately prior to filtration, an aliquot of each sample to measure $^{15}N_2$ enrichment in each bottle was transferred to a helium-flushed exetainer using a gas-tight syringe and preserved by adding 50 μl of a helium-flushed zinc chloride or mercuric chloride solution (50% w/v $ZnCl_2$ and $HgCl_2$, Thermo Fisher Scientific, Waltham, MA).

To establish the initial isotopic composition and concentration of PN in water samples, water from each depth sampled was collected separately. Triplicate samples were filtered at the time of collection in a designated laboratory space isolated from where experiments using ^{15}N tracer were being conducted to avoid isotope contamination. Filters for both initial and final PN analysis were placed in sterile microcentrifuge tubes and frozen until analysis at Old Dominion University. Filters were dried for 48 hr at 50 °C then pelletized in tin discs. PN and C concentrations and isotopic enrichment were measured using a Europa 20-20 isotope ratio mass spectrometer (IRMS) equipped with an automated N and C analyzer. Isotopic enrichment of dissolved N_2 was measured using a Europa 20-22 continuous flow IRMS, as described in Jayakumar et al. (2017).

2.3. NFR Calculations and Error Analysis

Volumetric NFR were calculated using equation (1):

$$NFR = \frac{A_{\mathrm{PN}_f} - A_{\mathrm{PN}_0}}{A_{N_2} - A_{\mathrm{PN}_0}} \times \frac{[PN]}{\Delta t} \quad (1)$$

where A_{PN_0}, A_{PN_f}, A_{N_2}, and [PN] represent the average initial and final PN isotopic composition, isotopic composition of the N_2 pool, and PN concentration of three replicate samples. The standard deviation of these replicates was propagated to calculate NFR error following Montoya et al. (1996) and Gradoville et al. (2017). The incubation time is denoted as Δt, and the uncertainty of this value was estimated based on the average time required to filter the given volume of seawater relative to the length of the incubation. A sensitivity analysis of the relative contributions of each measurement to total error is presented in Table S1. See supporting information Text S1 for further details on rate and error calculations.

A change in the atom percent enrichment of the PN pool was considered detectable if it exceeded 3 times the standard deviation of eight 12.5-μg N replicate standards which were run daily (Ripp, 1996). A LOD was calculated for each volumetric rate by substituting this value for $A_{\mathrm{PN}_f} - A_{\mathrm{PN}_0}$. A limit of quantification was similarly calculated by taking 10 times the standard deviation of the replicate standards (Ripp, 1996). The average LOD for PN mass, calculated based on blanks (3σ, $n = 4$), among all IRMS runs for this study was 0.83 μg N. This value, however, should not be confused with the minimum mass deemed acceptable for determination of isotope ratios. The accuracy of enrichment measurements decreases with decreasing mass (Sharp, 2017), and so a lower limit of acceptable mass was established per instrument run based on the linearity of the atom percent measured during each standard run; on average this was 3.0 μg N for this study. The mass of standards ranged from 1.17 to 100 μg N.

Areal (depth-integrated) rates were calculated for the euphotic zone (defined as the region extending from the surface to the 0.1% light level; Table 2) by averaging volumetric rates measured for the surface mixed layer, from the bottom of the surface mixed layer to the 1% light level, and from the 1% to 0.1% light level, then depth integrating over each layer and summing the respective contributions. If the volumetric rate at a given depth was below the LOD, then it was assigned a value of 0 nmol $N{\cdot}L^{-1}{\cdot}day^{-1}$ for the purpose of calculating the areal rate. If the calculated NFR was above the LOD but below the limit of quantification (i.e., it was detectable but not quantifiable), then the LOD was used in the areal rate calculation. The error associated with both nondetectable and nonquantifiable rates was propagated along with that of all quantifiable rates. NFR were not depth integrated in subeuphotic waters because quantifiable rates were sparse and accurate estimation of subeuphotic areal NFR consequently untenable. Areal NFR from the euphotic zone were compared between inshore (1 to 9) and offshore (10 to 16) stations using a two-tailed Mann-Whitney *U* test.

2.4. Carbon Addition Bioassays

Carbon addition bioassays were carried out at Stations 6, 9, 12, 15, and 16 at depths within and below the core ODZ to determine whether the supply of organic C limited NFR. For these experiments, samples were collected as described above. Once sealed, but prior to $^{15}N_2$ additions, one set of triplicate bottles was amended with glucose (Cambridge Isotopes, Tewksbury, MA) and another with a mixture of 20 amino acids (Cambridge Isotopes, Tewksbury, MA), resulting in a final addition of 40-μmol organic C/L to both sets of incubations. This addition approximately doubled the availability of dissolved organic C (Hansell & Carlson, 1998; Loh & Bauer, 2000), although much of the ambient dissolved organic C pool is thought to be very old and likely refractory (Druffel et al., 1992), thereby augmenting the significance of these C amendments to microbial communities present. Unamended triplicate incubations served as controls. Experimental treatments were compared to controls using a Wilcoxon signed-rank test. Where N_2 fixation was not detected or quantified, the lower limit of these values, zero or the LOD respectively, was used in statistical calculations. This approach increases our ability to detect significant differences (lower Type II error risk) but increases the probability of a false positive (higher Type I error risk).

3. Results and Discussion

3.1. Regional Hydrography

Surface waters of the ETNP are characterized by high productivity, a strong pycnocline that prevents local ventilation of deep waters, and a thermal front where the cool California Current meets the eastern Pacific warm pool (Fiedler & Talley, 2006). Our study area crossed this frontal region. Alongshore surface waters were cool to the north (<25 °C at Stations 1 to 4) and warmer south of the Gulf of California (Table 2 and Figure 2a). Surface waters at Stations 9 to 13 exceeded 27.5 °C, characteristic of the eastern Pacific warm pool (Fiedler & Talley, 2006), and salinity was low, below 34 (Table 2 and Figure 2b), suggestive of Tropical Surface Waters ($T > 25$, $S < 34$; Fiedler & Talley, 2006).

These waters typically exhibit little seasonal and ENSO variability in sea surface temperature and salinity; however, ENSO events are associated with a local deepening of the thermocline (Fiedler & Talley, 2006). In the present study, the thermocline shoaled and strengthened alongshore to the southeast (Figures 3i and 3j), following regional trends observed previously (Fiedler & Talley, 2006). The nitracline and primary chlorophyll *a* fluorescence maximum also shoaled to the southeast, accompanied by an increase in chlorophyll *a* fluorescence (Figures 3e–3h). A secondary chlorophyll *a* fluorescence maximum was evident at Stations 5 to 13, where the core ODZ was thickest and NO_2^- concentrations highest.

O_2-deficient waters, defined as those in which O_2 concentrations were below detection by the Seabird O_2 sensor (<3 μmol/kg) and NO_2^- concentrations were above 0.5 μM (Thamdrup et al., 2012), were observed at all offshore stations (10 to 16) and inshore Stations 5 to 9 along the west coast of Mexico (Figures 1b and 1c). The thickness of the ODZ increased toward the southeastern most station, expanding from 200 to 400 m at northerly Stations 15, 16, and 5, to a thickness of 100 to 600 m at Station 9. Stations 1 to 4 were north of the ODZ but exhibited suboxic (<20 μmol/kg O_2) conditions below the euphotic zone (Figures 3a–3d). The OMZ, the low-O_2 depth horizon present throughout the region, was characterized by slightly higher salinity (~34.7–34.8) and warmer temperatures (10–16 °C) relative to underlying waters (S ≈ 24.6–34.5, $T \leq 10$°C)

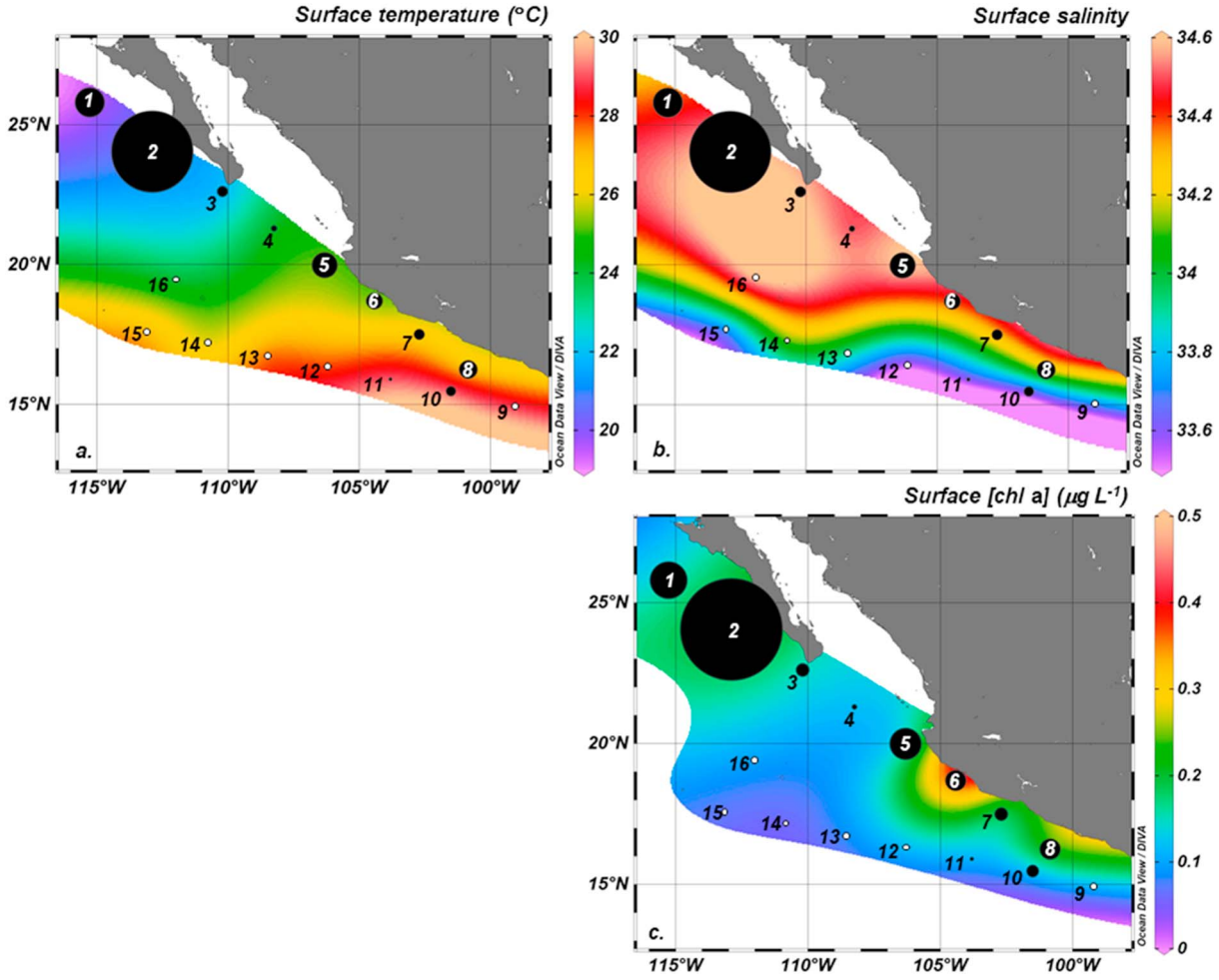

Figure 2. (a) Surface temperature (°C), (b) salinity, and (c) chlorophyll *a* concentration (μg/L) overlain by black dots sized to represent N_2 fixation rates depth integrated throughout the euphotic zone (see Table 2 for values). White dots depict locations where N_2 fixation was undetectable throughout the euphotic zone.

and higher salinity (Table S2) than the California Current water intruding from the north (Fiedler & Talley, 2006). DIN:SRP ratios remained within a narrow range (8.5 to 12) from below the thermocline to approximately 400 m then gradually increased, stabilizing near 14 after 1,000 m. In the North Pacific Ocean, DIN:SRP ratios are typically ~14.1, averaging 14.6 below 1,000 m (Tyrrell & Law, 1997).

3.2. N_2 Fixation in the Euphotic Zone

NFR were relatively high in the warm, sunlit, oxic waters (Figures 3k and 3l), where NO_3^- and SRP concentrations were low (Figures 3e, 3f, S1a, and S1b) and DIN:SRP was consistently below 3 (Figures S1c and S1d), suggestive of N_r limitation. N_2 fixation was detected in euphotic waters at 10 of the 16 stations, in 17 of 62 samples collected (Table S2). Most of these samples came from Stations 1 to 8 where surface salinity and concentrations of chlorophyll *a* and SRP were comparatively high (Figures 2b, 2c, S1a, and S1b). NFR were highest and extended deeper into the water column where the thermocline was weakest, constricting toward the southeast as the underlying ODZ shoaled (Figures 3a, 3b, 3k, and 3l and Table S2). Depth-integrated euphotic NFR among inshore stations (1 to 9) were significantly greater than at offshore stations (10 to 16; Mann Whitney U, $n_1 = 7$, $n_2 = 9$, $U = 93$, $p = 0.003$), ranging from below detection to 6,230 ± 5,500 μmol N·m^{-2}·day^{-1} (Table 2) with a median value among all measurable areal rates of 176 μmol N·m^{-2}·day^{-1}.

Recent work has focused on the potential for enhanced N_2 fixation along productive continental margins, particularly those in which low DIN:SRP waters are upwelled (e.g., Bonnet et al., 2013; Chang et al., 2019; Dekaezemacker et al., 2013; Deutsch et al., 2007; Fernandez et al., 2011; Jayakumar et al., 2017; Knapp

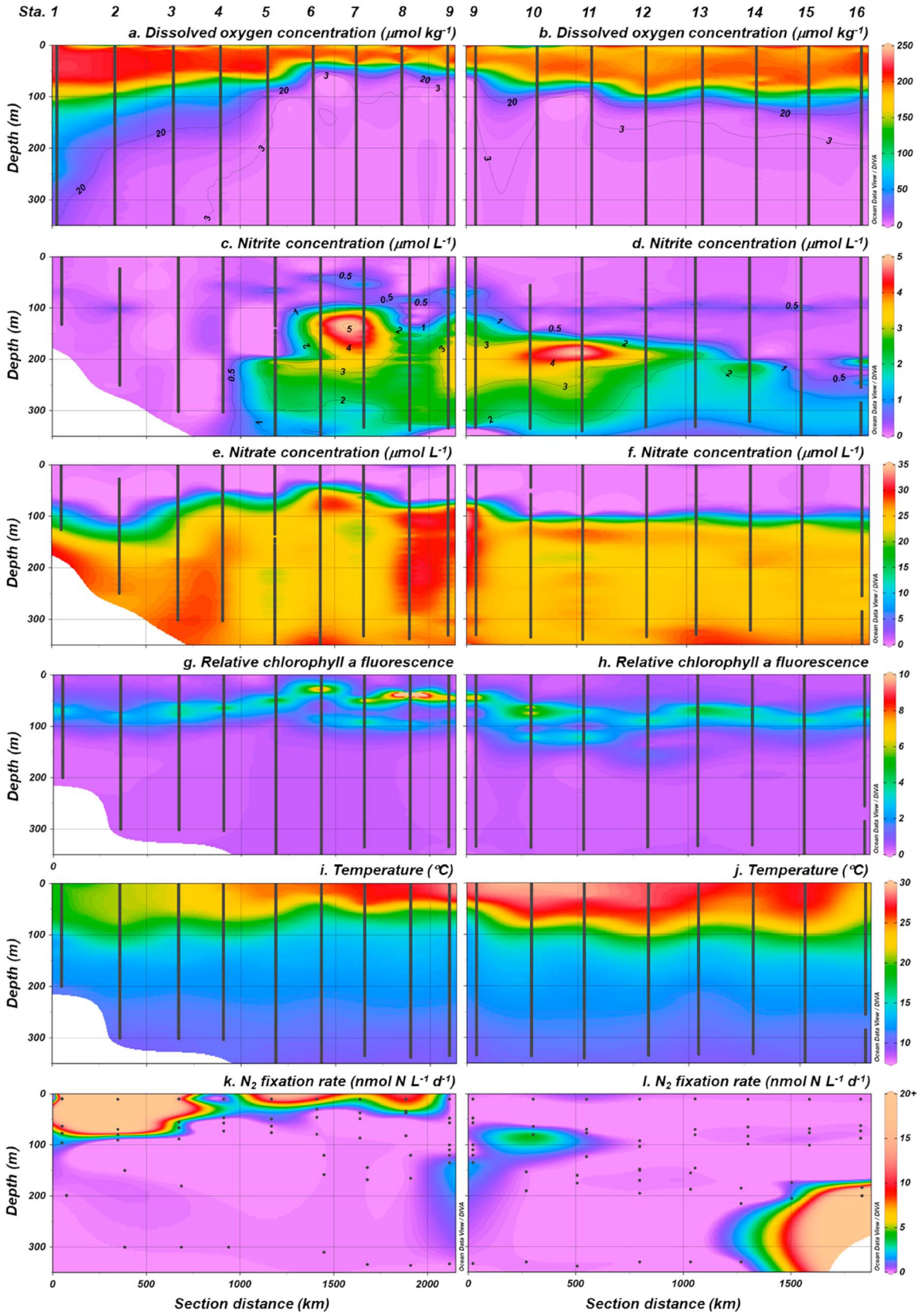

Figure 3. Hydrography (a–j) and N_2 fixation rates (k, l) in upper 350 m of inshore (left column) and offshore (right column) transects. Black lines and dots represent continuous or near-continuous profiles collected from the Pump Profiling System and discrete sampling points, respectively.

Table 2
Surface Hydrographic Characteristics and Depth-Integrated N_2 Fixation Rates Within the Euphotic Zone

Station	Latitude (°N)	Longitude (°W)	Surface temperature (°C)	Surface salinity	Euphotic zone depth (m)	Areal euphotic N_2 fixation rate (μmol N·m^{-2}·day^{-1})
1	25.791	−115.261	19.5	34.4	99	814 (396)
2	24.041	−112.891	21.0	34.6	114	6,226 (5,493)
3	22.608	−110.202	21.9	34.6	88	102 (30)
4	21.292	−108.242	24.3	34.5	107	14 (17)
5	19.985	−106.313	25.2	34.6	81	588 (108)
6	18.688	−104.416	25.3	34.4	65	250 (66)
7	17.500	−102.700	26.6	34.3	89	99 (29)
8	16.250	−100.845	27.0	34.2	69	257 (95)
9	15.000	−98.999	28.7	33.7	74	Not detected
10	15.469	−101.502	29.2	33.6	94	85 (41)
11	15.901	−103.799	29.1	33.6	110	7 (21)
12	16.315	−106.091	28.0	33.5	107	Not detected
13	16.778	−108.398	27.7	33.9	108	Not detected
14	17.204	−110.712	25.9	34.1	111	Not detected
15	17.625	−113.001	27.0	33.7	117	Not detected
16	19.508	−111.895	24.0	34.6	118	Not detected

Note. Rate measurement propagated error, calculated as described in section 2, is given in parentheses.

et al., 2016; Loescher et al., 2014; Sohm et al., 2011; White et al., 2013). Comparison of these systems to N_r-deplete ocean gyres, where the bulk of global N_2 fixation has historically been ascribed, is, however, complicated by methodological biases—chiefly, the potential underestimation of the classic $^{15}N_2$ bubble method due to the slow dissolution of $^{15}N_2$ (Böttjer et al., 2017; Großkopf et al., 2012; Mohr et al., 2010), as well as underestimation or overestimation of N_2 fixation when measured indirectly via the acetylene reduction assay (Mulholland et al., 2004). Luo et al. (2012) calculated an arithmetic mean areal NFR for North Pacific (0°N to 55°N) euphotic zone of 120 ± 22 μmol N·m^{-2}·day^{-1} based on studies applying these methods primarily in the basin's interior. Böttjer et al. (2017) accounted for the approximately twofold underestimation of the $^{15}N_2$ bubble method in time series data from station ALOHA (North Pacific subtropical gyre) and calculated an average rate of 230 ± 136 μmol N·m^{-2}·day^{-1}. These values are in relatively good agreement if a correction factor of 2 (Böttjer et al., 2017; Großkopf et al., 2012) is also applied to Luo and colleague's basin-wide estimate.

Of the 10 stations where N_2 fixation was detected in surface waters for this study, areal rates exceeded the station ALOHA mean (Böttjer et al., 2017) at five—all located near the coastline (Table 2). If, however, we account for the error inherent to the areal rates presented in this study and variation from the mean at station ALOHA, only rates at Stations 1, 2, and 5 clearly exceed mean N_2 fixation at station ALOHA, and only at Stations 1 and 2 does N_2 fixation exceed the maximum rate at ALOHA where NFR range from 21 to 676 μmol N·m^{-2}·day^{-1} (Böttjer et al., 2017). Nevertheless, the observed distribution of euphotic zone N_2 fixation in this study and the elevation of these rates above the regional average suggest that conditions in the cooler, saltier, more productive water mass near the continent favored the growth and activity of local diazotroph communities relative to those in the central North Pacific basin. This finding supports the observation of Jayakumar et al. (2017) that euphotic, inshore NFR in the ETNP ODZ region exceeded those offshore.

Euphotic NFR reported here (with a median value of 176 μmol N·m^{-2}·day^{-1}) were also high relative to waters overlying the ETSP ODZ, where Bonnet et al. (2013) and Fernandez et al. (2011) estimate average areal rates of 43 ± 6 and 48 ± 68 μmol N·m^{-2}·day^{-1}, respectively, using the classic $^{15}N_2$ bubble method. These values are in relatively good agreement with other incubation-based estimates from the ETSP euphotic zone (Dekaezemacker et al., 2013; Knapp et al., 2016) and are comparable to those observed in the central South Pacific gyre (94 ± 61 μmol N·m^{-2}·day^{-1}; Halm et al., 2012), indicating that surface waters of the ETSP ODZ do not support elevated NFR as predicted by Deutsch et al. (2007). Despite these low regional means, Loescher et al. (2014) observed N_2 fixation to exceed 800 μmol N·m^{-2}·day^{-1} at one coastal sulfidic station in the ETSP, suggesting that sulfidic events may sporadically enhance rates. Nevertheless, N_2 fixation is thought to be only a minor contributor of N_r to export production in the ETSP (Chang et al., 2019; Knapp et al., 2016).

N_2 fixation may be greater in ETNP surface waters relative to those of the ETSP because the North Pacific receives higher aeolian Fe inputs (Jickells et al., 2005). Indeed, Fe amendments have been observed to increase NFR in ETSP surface waters (Dekaezemacker et al., 2013). It must be noted, however, that the present study occurred during an ENSO event, which has been associated with enhanced NFR in the ETSP (Dekaezemacker et al., 2013). Further work is therefore necessary to elucidate whether this event affected N_2 fixation in the ETNP and consequently whether these regional differences are truly significant.

High rates of N_2 fixation—on par with those observed here at Stations 1, 2, and 5 (Table 2)—have also been observed along other ocean margins (e.g., Carpenter et al., 1999; Mulholland et al., 2012, 2014; Rees et al., 2009; Shiozaki et al., 2015; Wen et al., 2017) including areas characterized by low concentrations of DIN relative to SRP and other essential elements (e.g., Fe, silicon for diatom-diazotroph symbioses) resulting from riverine inputs (Grosse et al., 2010; Subramaniam et al., 2008) and advection of ODZ-generated N_r-deplete waters into marginal seas (White et al., 2013). In the Amazon River plume and Gulf of California, the latter of which receives N_r-deplete waters from the ETNP ODZ via the California Undercurrent, areal NFR as high as ~8,000 μmol $N{\cdot}m^{-2}{\cdot}day^{-1}$ (Subramaniam et al., 2008) and ~900 μmol $N{\cdot}m^{-2}{\cdot}day^{-1}$ (White et al., 2013) have been reported, respectively. Along the Southern New England shelf, NFR reached 4,106 μmol $N{\cdot}m^{-2}{\cdot}day^{-1}$ in Fall (Mulholland et al., 2019). In euphotic waters of the Benguela Upwelling System, another eastern boundary upwelling system predicted by Deutsch et al. (2007) to support elevated N_2 fixation, rates were far lower but increased inshore (Sohm et al., 2011) as observed in this study. These findings, along with the present study, suggest that diazotroph activity is heightened along ocean margins, particularly where N_r is drawn down relative to SRP and other nutrients as occurs in the ETNP (Table 2).

Proximity to the continent likely offers advantages to some diazotrophic groups relative to others, depending on the physical and chemical properties of the water column, their metabolic requirements, and genetic capabilities. Enhanced availability of organic C in productive inshore waters may provide energy to heterotrophic diazotrophs and low-oxygen/anoxic microzones for noncyanobacterial diazotrophs fixing N_2 in fully oxic waters (Bombar et al., 2016), such as those observed in the ETNP and ETSP ODZs (Chang et al., 2019; Jayakumar et al., 2017). Indeed, sinking particles have been identified as loci of both cyanobacterial and noncyanobacterial diazotrophs in the North Pacific subtropical gyre (Farnelid et al., 2019). Additionally, Fe can be delivered to the ocean from the continents via aeolian transport and riverine inputs (Hunter & Boyd, 2007), the latter of which may also serve as a source of Fe-binding ligands (e.g., Bundy et al., 2015; Laglera & van den Berg, 2009) that maintain dissolved Fe in solution (Rue & Bruland, 1995; van den Berg, 1995).

3.3. Subeuphotic N_2 Fixation and Carbon Limitation

Within OMZ waters, NFR were detected at 3 of the 16 stations (Stations 9, 15, and 16), within 5 of the 39 samples collected at this depth horizon—all of which were from suboxic (<20 μmol/kg O_2) waters (Table S2). Within the OMZ at Stations 9 and 15, the highest volumetric rates were 1.55 ± 0.41 nmol $N{\cdot}m^{-2}{\cdot}day^{-1}$ (Station 9 at 135 m, $n = 3$) and 1.01 ± 1.34 nmol $N{\cdot}m^{-2}{\cdot}day^{-1}$ (Station 15 at 174 m, $n = 3$), respectively. Of the four stations (6, 9, 12, and 16) where NFR were measured in samples collected below the ODZ (≥500 m), rates were only detected at Stations 9 and 16 and were lower than measurable rates within the ODZ at these sites (Figure 4). O_2 concentrations at these stations remained low, below 150 μmol/kg, even in deep waters (Table S2). At Station 9, a NFR of 0.87 ± 0.99 nmol $N{\cdot}m^{-2}{\cdot}day^{-1}$ ($n = 3$) was measured at 1,000 m; N_2 fixation was detectable but not quantifiable at 2,000 m. Rates at station 16 exceeded those measured elsewhere by about an order of magnitude (9.88 ± 3.85 nmol $N{\cdot}m^{-2}{\cdot}day^{-1}$ at 184 m and 35.9 ± 12.0 nmol $N{\cdot}m^{-2}{\cdot}day^{-1}$ at 200 m, $n = 3$), peaking at the top of the ODZ but remaining quantifiable to 3,000 m (0.36 ± 0.15 nmol $N{\cdot}m^{-2}{\cdot}day^{-1}$, $n = 3$; Figure 4).

If low-O_2 conditions within the water column favor N_2 fixation, then one would expect NFR to be commensurately higher within and around the ODZ than in other oceanic environments. Both within and below the OMZ at all sites, however, NFR appeared patchy. Of the 51 subeuphotic samples collected, N_2 fixation was only detected in 10 (Table S2), and 5 of these were from one station, 16, located near the inner Revillagigedo Islands. NFR previously reported in oxygenated, aphotic marine waters are typically on the order of 1 nmol $N{\cdot}L^{-1}{\cdot}day^{-1}$ or lower (Moisander et al., 2017, and references therein). This rate is comparable with measurements presented here from within and below the ETNP OMZ including in ODZ waters, except for at station

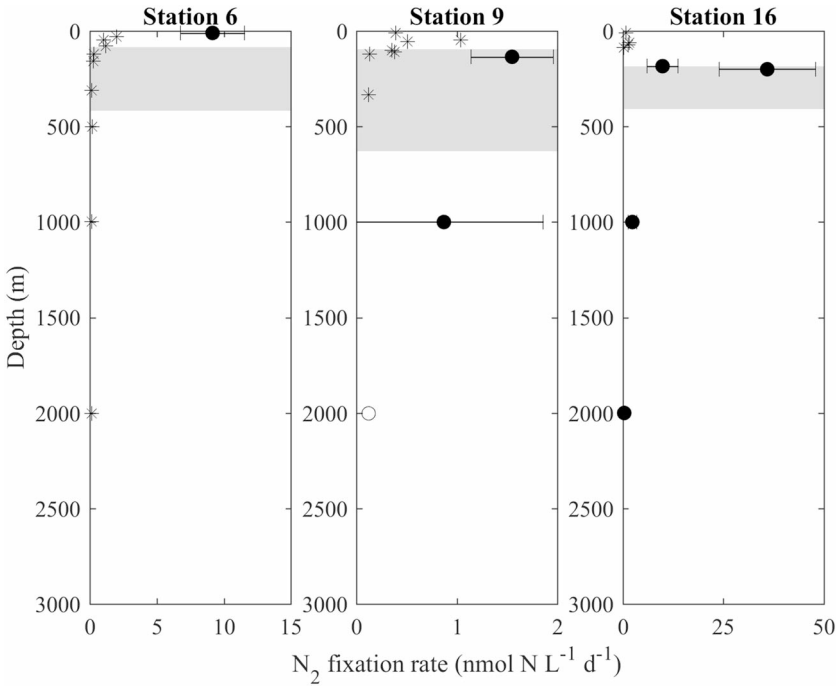

Figure 4. Profiles of N_2 fixation at stations 6 (inshore), 9 (southerly), and 16 (northerly, offshore). Black stars, open circles, and filled circles represent rates that were below detection, detectable but nonquantifiable, and quantifiable. For rate measurements below detection, the limit of detection was plotted; for nonquantifiable rates, the limit of quantification was plotted. Error bars for quantifiable rates represent the propagated error. The shaded region represents where core oxygen deficient zone conditions (O_2 concentrations below detection and >0.5-μM NO_2^-) occurred. A deep profile of N_2 fixation rates was also produced at station 12 (offshore); however, no N_2 fixation was detected at this site (Table S2).

16 (Table S2 and Figure 4), suggesting that suboxic/anoxic conditions alone do not result in elevated subeuphotic N_2 fixation in this region. This appraisal is consistent with work from Jayakumar et al. (2017) who previously observed few low rates (<1 nmol $N{\cdot}L^{-1}{\cdot}day^{-1}$) of N_2 fixation within the upper ETNP ODZ.

The patchy distribution of subeuphotic N_2 fixation presented here contrasts with some observations from the ETSP ODZ. In the ETSP, Bonnet et al. (2013) reported that low (<1 nmol $N{\cdot}L^{-1}{\cdot}day^{-1}$) but persistent rates below the euphotic zone account for ~90% of total N_2 fixation. Similarly, Fernandez et al. (2011) estimated that the ODZ contributed about 5 times as much newly fixed N as oxic, euphotic waters. More recent work from Chang et al. (2019), which applied the same $^{15}N_2$ bubble removal method as this study, diverges from these accounts. Chang et al. (2019) found no detectable NFR below the euphotic zone. This stark difference may be partially the result of methodological disparities, including the erroneous assumption in earlier ODZ work (e.g., Fernandez et al., 2011) that atom percent ^{15}N of the initial PN pool is equivalent to atmospheric values, which may inflate reported rate measurements (Chang et al., 2019; Voss et al., 2001). Whether the subeuphotic environment contributes significantly to total regional N_r inputs also depends upon the manner in which detection limits are calculated given that even very small rates may be substantive when depth integrated through a deep water column. Regardless, NFR measurements in subeuphotic ETSP waters are largely within the range of those observed elsewhere in the ocean's interior (≤1 nmol $N{\cdot}L^{-1}{\cdot}day^{-1}$; Moisander et al., 2017, and references therein) and generally appear less patchy than those reported here from the ETNP.

Though NFR were undetectable throughout most of the ETNP OMZ, dissolved organic C additions of either glucose or dissolved free amino acids (DFAA) stimulated N_2 fixation within all OMZ waters surveyed, including within the ODZ at Stations 6 and 12 where NFR were otherwise undetectable (Figure 5a). This finding indicates that the ETNP OMZ hosts populations of diazotrophs capable of fixing N_2 in suboxic and anoxic waters, despite significant concentrations of ambient DIN. Additions largely failed to stimulate N_2 fixation below the OMZ (Figure 5b). As energy-rich molecules, DFAA and glucose may enter both

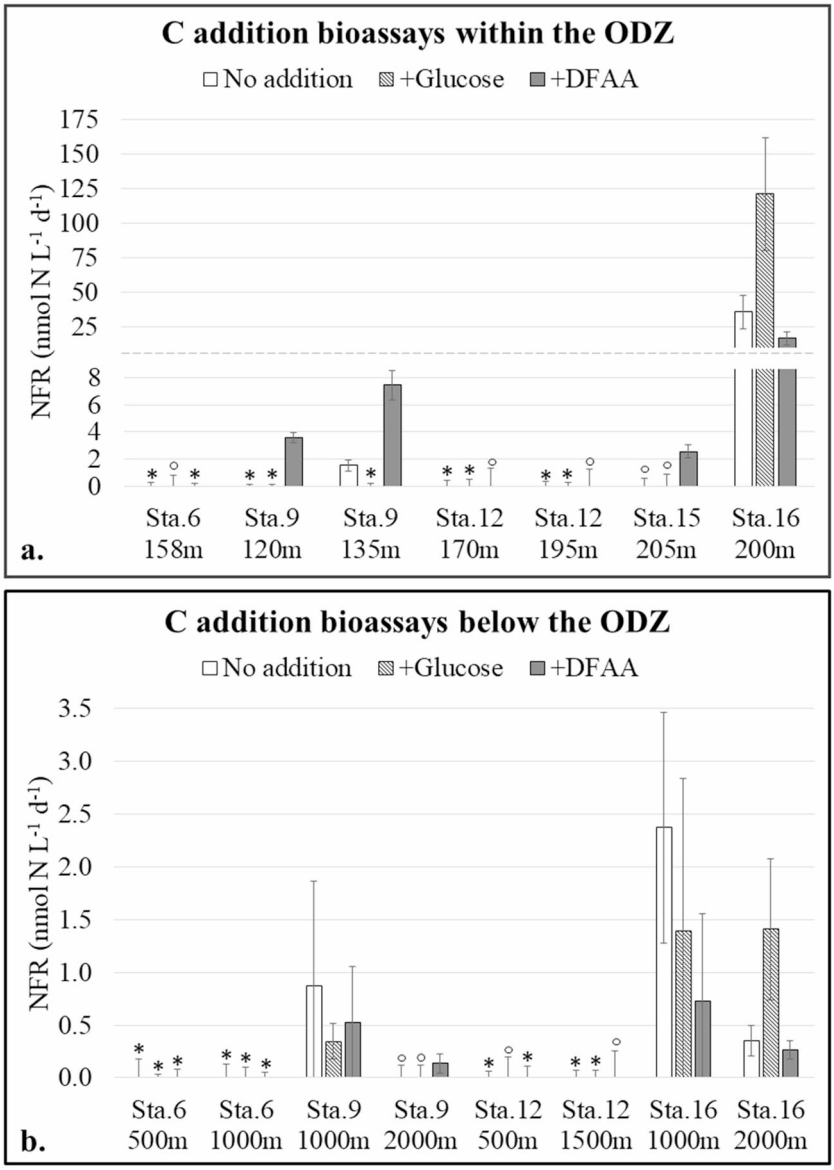

Figure 5. Results of carbon addition bioassay experiments within (a) and below (b) the O_2 minimum zone. Nitrogen fixation rates (NFR) marked with an open circle were detectable but not quantifiable. Stars indicate rates that were below the detection limit. For quantifiable rates, error bars express the propagated error. For DNQ rates, error bars express the limit of quantification calculated for that sample. Where no N_2 fixation was detected, the error bar marks the limit of detection. Neither additions of glucose nor dissolved free amino acids (DFAA) increased rates within ($n_1 = n_2 = 7$) or below ($n_1 = n_2 = 8$) the O_2 minimum zone significantly when compared across all sites (Wilcoxon signed rank, $p > 0.05$). ODZ = oxygen deficient zone.

catabolic and anabolic pathways. Consequently, our findings could indicate that diazotrophic activity within the OMZ is limited by either energy or assimilable C.

DFAA additions stimulated NFR at five of seven sampling locations within the OMZ, although this lacked statistical significance when compared across all sites (Wilcoxon signed rank, $n_1 = n_2 = 7$, $p = 0.44$), potentially due to the small sample size. Conversely, DFAA additions inhibited while glucose additions stimulated rates at certain depths at Station 16 (Figure 5). Within the ETSP ODZ, Bonnet et al. (2013) found that DFAA additions stimulated N_2 fixation in all ODZ waters surveyed while mixed carbohydrate or glucose additions only stimulated N_2 fixation at one third of the stations surveyed. DFAA additions also enhanced N_2 fixation in the Red Sea (Rahav et al., 2013, 2015) and mesopelagic waters of the southwest Pacific Ocean (Benavides

et al., 2015). These observations are perhaps surprising given that DFAA offer a source of N as well as C for heterotrophs and might thus be expected to suppress NFR. If, however, DFAA were used in catabolic rather than anabolic (assimilatory) processes, organic N might be excreted in the form of a waste product. We hypothesize that site-specific differences in microbial response to DFAA and glucose additions are due to population-specific substrate preferences, variability in energy/C limitation, or both. Regarding the response of diazotrophic communities below the OMZ, lower temperatures can slow bacterial metabolic rates (Price & Sowers, 2004) and decrease affinity for organic substrates (Nedwell, 1999). The response of any diazotrophs present in deep waters may consequently have been dampened within the timeframe of incubations, or there are no diazotrophs present and active at this depth.

Our findings suggest that diazotrophs inhabit the ETNP region and fix N_2 at elevated rates in euphotic waters near the coast but are largely inactive in OMZ and ODZ waters, as well as in the water column below, likely due to energy or C limitation at the OMZ depth horizon. In subeuphotic waters, detectable NFR were mostly on par with previous reports from oxygenated aphotic ocean waters (Moisander et al., 2017, and references therein). High NFR were, however, observed within suboxic waters at one station, 16, located near volcanic islands, suggesting that noncyanobacterial diazotrophs may thrive in DIN-replete waters given the right conditions. Here, NFR were highest in suboxic waters and decreased below the ODZ (Figure 4) following increased O_2 concentrations (Table S2) and decreased provision of organic C given that particulate C fluxes decrease with depth (Martin et al., 1987). High-carbon/low-oxygen conditions have previously been associated with increased activity of noncyanobacterial diazotrophs (Severin et al., 2015), and further investigation into how these factors may affect the range and magnitude of noncyanobacterial N_2 fixation is warranted.

4. Conclusions

Here, we present the most extensive data set to date of N_2 fixation above, within, and below the ETNP ODZ. Our observation of high rates (>500 μmol $N \cdot m^{-2} \cdot day^{-1}$) at inshore stations supports the growing body of evidence that ocean margins contribute a greater amount of newly fixed N than previously thought (Mulholland et al., 2019; Tang et al., 2019). We hypothesize that continental inputs, inshore upwelling, or both alleviate growth limitation by an essential factor and play a key role in shaping the distribution of diazotrophs in N_r-deplete waters regionally. Furthermore, we speculate that diazotrophs residing near the coast (this study) and in marginal seas (White et al., 2013) where N_r-deplete waters upwell are important to basin-scale compensation of N_r deficits generated in the ETNP ODZ and merit further investigation.

This study also demonstrates that subeuphotic, suboxic waters in the region harbor diazotrophs capable of fixing N_2 despite high (>20 μmol $N \cdot L^{-1} \cdot day^{-1}$) ambient DIN concentrations, but their activity is highly patchy and appears C limited. While it is known that ambient DIN does not necessarily preclude N_2 fixation (Knapp, 2012), the observation of relatively high NFR (>9 nmol $N \cdot L^{-1} \cdot day^{-1}$) in DIN-replete deep waters challenges the prevailing hypothesis that N cycle homeostasis is maintained, in part, by the occurrence of N_2 fixation where N_r is drawn down (Deutsch et al., 2007; Weber & Deutsch, 2014). Further work is needed to elucidate the response of diverse diazotrophic communities to DIN. Despite observation of patchy but high rates within and around the ETNP ODZ, N_2 fixation throughout the region appears too low to compensate for local N_r losses. This finding adds to the mounting evidence that N_r inputs and losses are spatially decoupled (Bonnet et al., 2013, 2017; Knapp et al., 2016, 2018; Weber & Deutsch, 2014). By elucidating the distribution of N_2 fixation across physico-chemical gradients in an undersampled but biogeochemically important region, this study contributes to our evolving understanding of the factors that regulate marine N_2 fixation and the ocean's N_r inventory.

Acknowledgments
We gratefully acknowledge the efforts of the captain and crew of the NOAA vessel *Ronald H. Brown* and the scientists who participated in the collection and analysis of the data presented here, particularly Shannon Cofield, Wei Yan, Nicole Travis, and Matt Forbes. We thank the Monterey Bay Aquatic Research Institute for the use of their pump profiling system and Margeurite Blum for her expertise in its use. Finally, we thank Bess Ward for the use of her facilities at Princeton University. This work was supported by the National Science Foundation Division of Ocean Sciences (NSF-OCE) Grant OCE-1356056 to M. R. M. and A. J. Data will be made available at the website (https://www.bco-dmo.org/project/472492). The authors declare no conflicts of interest.

References

Andersson, B., Sundbäck, K., Hellman, M., Hallin, S., & Alsterberg, C. (2014). Nitrogen fixation in shallow-water sediments: Spatial distribution and controlling factors. *Limnology and Oceanography*, *59*(6), 1932–1944. https://doi.org/10.4319/lo.2014.59.6.1932

Benavides, M., Bonnet, S., Hernández, N., Martínez-Pérez, A. M., Nieto-Cid, M., Álvarez-Salgado, X. A., et al. (2016). Basin-wide N_2 fixation in the deep waters of the Mediterranean Sea. *Global Biogeochemical Cycles*, *30*, 952–961. http://doi.org/10.1002/2015GB005326

Benavides, M., Moisander, P. H., Berthelot, H., Dittmar, T., Grosso, O., & Bonnet, S. (2015). Mesopelagic N_2 fixation related to organic matter composition in the Solomon and Bismarck Seas (Southwest Pacific). *PLoS ONE*, *10*(12), e0143775. https://doi.org/10.1371/journal.pone.0143775

Bentzon-Tilia, M., Traving, S. J., Mantikci, M., Knudsen-Leerbeck, H., Hansen, J. L., Markager, S., & Riemann, L. (2015). Significant N_2 fixation by heterotrophs, photoheterotrophs and heterocystous cyanobacteria in two temperate estuaries. *The ISME Journal*, *9*(2), 273–285. https://doi.org/10.1038/ismej.2014.119

Berges, J. A., & Mulholland, M. R. (2008). Enzymes and nitrogen cycling. In D. G. Capone, D. A. Bronk, M. R. Mulholland, & E. J. Carpenter (Eds.), *Nitrogen in the marine environment* (2nd ed., pp. 1385–1444). Waltham, MA: Academic Press. https://doi.org/10.1016/B978-0-12-372522-6.00032-3

Blais, M., Tremblay, J. É., Jungblut, A. D., Gagnon, J., Martin, J., Thaler, M., & Lovejoy, C. (2012). Nitrogen fixation and identification of potential diazotrophs in the Canadian Arctic. *Global Biogeochemical Cycles*, *26*, GB3022. http://doi.org/10.1029/2011GB004096

Bombar, D., Paerl, R. W., & Riemann, L. (2016). Marine non-cyanobacterial diazotrophs: moving beyond molecular detection. *Trends in Microbiology*, *24*(11), 916–927. https://doi.org/10.1016/j.tim.2016.07.002

Bonnet, S., Caffin, M., Berthelot, H., & Moutin, T. (2017). Hot spot of N_2 fixation in the western tropical South Pacific pleads for a spatial decoupling between N_2 fixation and denitrification. *Proceedings of the National Academy of Sciences*, *114*(14), E2800–E2801. https://doi.org/10.1073/pnas.1619514114

Bonnet, S., Dekaezemacker, J., Turk-Kubo, K. A., Moutin, T., Hamersley, R. M., Grosso, O., et al. (2013). Aphotic N_2 fixation in the eastern tropical South Pacific Ocean. *PLoS ONE*, *8*(12), e81265. https://doi.org/10.1371/journal.pone.0081265

Böttjer, D., Dore, J. E., Karl, D. M., Letelier, R. M., Mahaffey, C., Wilson, S. T., et al. (2017). Temporal variability of nitrogen fixation and particulate nitrogen export at Station ALOHA. *Limnology and Oceanography*, *62*(1), 200–216. https://doi.org/10.1002/lno.10386

Bundy, R. M., Abdulla, H. A., Hatcher, P. G., Biller, D. V., Buck, K. N., & Barbeau, K. A. (2015). Iron-binding ligands and humic substances in the San Francisco Bay estuary and estuarine-influenced shelf regions of coastal California. *Marine Chemistry*, *173*, 183–194. https://doi.org/10/1016/j/marchem/2014/11/005

Caputo, A., Stenegren, M., Pernice, M. C., & Foster, R. A. (2018). A short comparison of two marine planktonic diazotrophic symbioses highlights an un-quantified disparity. *Frontiers in Marine Science*, *5*, 2. http://doi.org/10.3389/fmars.2018.00002

Carpenter, E. J., & Capone, D. G. (2008). Nitrogen fixation in the marine environment. In D. G. Capone, D. A. Bronk, M. R. Mulholland, & E. J. Carpenter (Eds.), *Nitrogen in the marine environment*, (2nd ed., pp. 141–198). Waltham, MA: Academic Press. https://doi.org/10.1016/B978-0-12-372522-6.00004-9

Carpenter, E. J., Montoya, J. P., Burns, J., Mulholland, M. R., Subramaniam, A., & Capone, D. G. (1999). Extensive bloom of a N_2-fixing diatom/cyanobacterial association in the tropical Atlantic Ocean. *Marine Ecology Progress Series*, *185*, 273–283. https://doi.org/10.3354/meps185273

Chang, B. X., Jayakumar, A., Widner, B., Bernhardt, P., Mordy, C. W., Mulholland, M. R., & Ward, B. B. (2019). Low rates of dinitrogen fixation in the eastern tropical South Pacific. *Limnology and Oceanography*. http://doi.org/10.1002/lno.11159

Climate Prediction Center (2019). Historical El Niño/La Niña episodes (1950-present). http://origin.cpc.ncep.noaa.gov/products/analysis_monitoring/ensostuff/ONI_v5.php (21 January 2019, date last accessed).

Dabundo, R., Lehmann, M. F., Treibergs, L., Tobias, C. R., Altabet, M. A., Moisander, P. H., & Granger, J. (2014). The contamination of commercial $^{15}N_2$ gas stocks with ^{15}N-labeled nitrate and ammonium and consequences for nitrogen fixation measurements. *PLoS ONE*, *9*(10), e110335. https://doi.org/10.1371/journal.pone.0110335

Dekaezemacker, J., Bonnet, S., Grosso, O., Moutin, T., Bressac, M., & Capone, D. (2013). Evidence of active dinitrogen fixation in surface waters of the eastern tropical South Pacific during El Niño and La Niña events and evaluation of its potential nutrient controls. *Global Biogeochemical Cycles*, *27*, 768–779. http://doi.org/10.1002/gbc.20063

Deutsch, C., Sarmiento, J. L., Sigman, D. M., Gruber, N., & Dunne, J. P. (2007). Spatial coupling of nitrogen inputs and losses in the ocean. *Nature*, *445*(7124), 163–167. https://doi.org/10.1038/nature05392

DeVries, T., Deutsch, C., Primeau, F., Chang, B., & Devol, A. (2012). Global rates of water-column denitrification derived from nitrogen gas measurements. *Nature Geoscience*, *5*(8), 547–550. https://doi.org/10.1038/ngeo1515

Dixon, R., & Kahn, D. (2004). Genetic regulation of biological nitrogen fixation. *Nature Reviews Microbiology*, *2*(8), 621–631. https://doi.org/10.1038/nrmicro954

Druffel, E. R., Williams, P. M., Bauer, J. E., & Ertel, J. R. (1992). Cycling of dissolved and particulate organic matter in the open ocean. *Journal of Geophysical Research*, *97*(C10), 15639–15659.

Farnelid, H., Bentzon-Tilia, M., Andersson, A. F., Bertilsson, S., Jost, G., Labrenz, M., et al. (2013). Active nitrogen-fixing heterotrophic bacteria at and below the chemocline of the central Baltic Sea. *The ISME Journal*, *7*(7), 1413–1423. https://doi.org/10.1038/ismej.2013.26

Falkowski, P. G. (1983). Enzymology of nitrogen assimilation. In E. J. Carpenter & D. G. Capone (Eds.), *Nitrogen in the marine environment* (1st ed., pp. 839–868). New York, NY: Academic Press Inc.

Farnelid, H., Turk-Kubo, K., Ploug, H., Ossolinski, J. E., Collins, J. R., Van Mooy, B. A., & Zehr, J. P. (2019). Diverse diazotrophs are present on sinking particles in the North Pacific Subtropical Gyre. *The ISME Journal*, *13*(1), 170–182. https://doi.org/10.1038/s41396-018-0259-x

Fernandez, C., Farías, L., & Ulloa, O. (2011). Nitrogen fixation in denitrified marine waters. *PLoS ONE*, *6*(6), e20539. https://doi.org/10.1371/journal.pone.0020539

Fiedler, P. C., & Talley, L. D. (2006). Hydrography of the eastern tropical Pacific: A review. *Progress in Oceanography*, *69*(2-4), 143–180. https://doi.org/10.1016/j.pocean.2006.03.008

Flores, E., & Herrero, A. (2005). Nitrogen assimilation and nitrogen control in cyanobacteria. *Biochemical Society Transactions*, *33*(1), 164–167. https://doi.org/10.1042/BST0330164

Gradoville, M. R., Bombar, D., Crump, B. C., Letelier, R. M., Zehr, J. P., & White, A. E. (2017). Diversity and activity of nitrogen-fixing communities across ocean basins. *Limnology and Oceanography*, *62*(5), 1895–1909. https://doi.org/10.1002/lno.10542

Grosse, J., Bombar, D., Doan, H. N., Nguyen, L. N., & Voss, M. (2010). The Mekong River plume fuels nitrogen fixation and determines phytoplankton species distribution in the South China Sea during low and high discharge season. *Limnology and Oceanography*, *55*(4), 1668–1680. https://doi.org/10.4319/lo.2010.55.4.1668

Großkopf, T., & LaRoche, J. (2012). Direct and indirect costs of dinitrogen fixation in Crocosphaera watsonii WH8501 and possible implications for the nitrogen cycle. *Frontiers in Microbiology*, *3*, 236. http://doi.org/10.3389/fmicb.2012.00236

Großkopf, T., Mohr, W., Baustian, T., Schunck, H., Gill, D., Kuypers, M. M., et al. (2012). Doubling of marine dinitrogen-fixation rates based on direct measurements. *Nature*, *488*, 361–364. https://doi.org/10.1038/nature11338

Gruber, N., & Galloway, J. N. (2008). An Earth-system perspective of the global nitrogen cycle. *Nature*, *451*(7176), 293–296. https://doi.org/10.1038/nature06592

Halm, H., Lam, P., Ferdelman, T. G., Lavik, G., Dittmar, T., LaRoche, J., et al. (2012). Heterotrophic organisms dominate nitrogen fixation in the South Pacific Gyre. *The ISME Journal*, *6*, 1238–1249. http://doi.org/10.1038/ismej.2011.182

Hamersley, M. R., Turk, K. A., Leinweber, A., Gruber, N., Zehr, J. P., Gunderson, T., & Capone, D. (2011). Nitrogen fixation within the water column associated with two hypoxic basins in the Southern California Bight. *Aquatic Microbial Ecology*, *63*(2), 193–205.

Hansell, D. A., & Carlson, C. A. (1998). Deep-ocean gradients in the concentration of dissolved organic carbon. *Nature*, *395*, 263–266.

Harding, K., Turk-Kubo, K. A., Sipler, R. E., Mills, M. M., Bronk, D. A., & Zehr, J. P. (2018). Symbiotic unicellular cyanobacteria fix nitrogen in the Arctic Ocean. *Proceedings of the National Academy of Sciences*, *115*(52), 13,371–13,375.

Holmes, R. M., Aminot, A., Kérouel, R., Hooker, B. A., & Peterson, B. J. (1999). A simple and precise method for measuring ammonium in marine and freshwater ecosystems. *Canadian Journal of Fisheries and Aquatic Sciences*, *56*(10), 1801–1808. https://doi.org/10.1139/f99-128

Hunter, K. A., & Boyd, P. W. (2007). Iron-binding ligands and their role in the ocean biogeochemistry of iron. *Environmental Chemistry*, *4*, 221–232. https://doi.org/10.1071/EN07012

Jayakumar, A., Al-Rshaidat, M. M., Ward, B. B., & Mulholland, M. R. (2012). Diversity, distribution, and expression of diazotroph nifH genes in oxygen-deficient waters of the Arabian Sea. *FEMS Microbiology Ecology*, *82*(3), 597–606. https://doi.org/10.1111/j.1574-6941.2012.01430.x

Jayakumar, A., Chang, B. X., Widner, B., Bernhardt, P., Mulholland, M. R., & Ward, B. B. (2017). Biological nitrogen fixation in the oxygen-minimum region of the eastern tropical North Pacific Ocean. *The ISME Journal*, *11*(10), 2356–2367. https://doi.org/10.1038/ismej.2017.97

Jickells, T., An, Z., Andersen, K. K., Baker, A., Bergametti, G., Brooks, N., et al. (2005). Global iron connections between desert dust, ocean biogeochemistry, and climate. *Science*, *308*(5718), 67–71. https://doi.org/10.1126/science.1105959

Karl, D., Church, M., Dore, J., Letelier, R., & Mahaffey, C. (2012). Predictable and efficient carbon sequestration in the North Pacific Ocean supported by symbiotic nitrogen fixation. *Proceedings of the National Academy of Sciences*, *109*(6), 1842–1849. http://doi.org/10.1073/pnas.1120312109

Karl, D., Michaels, A., Bergman, B., Capone, D., Carpenter, E., Letelier, R., et al. (2002). Dinitrogen fixation in the world's oceans. In E. W. Boyer, & R. W. Howarth (Eds.), *The nitrogen cycle at regional to global scales* (pp. 47–98). Dordrect: Springer.

Knapp, A., Mccabe, K., Grosso, O., Leblond, N., Moutin, T., & Bonnet, S. (2018). Distribution and rates of nitrogen fixation in the western tropical South Pacific Ocean constrained by nitrogen isotope budgets. *Biogeosciences*, *15*(9), 2619–2628. https://doi.org/10.5194/bg-15-2619-2018

Knapp, A. N. (2012). The sensitivity of marine N_2 fixation to dissolved inorganic nitrogen. *Frontiers in Microbiology*, *3*. https://doi.org/10.3389/fmicb.2012.00374

Knapp, A. N., Casciotti, K. L., Berelson, W. M., Prokopenko, M. G., & Capone, D. G. (2016). Low rates of nitrogen fixation in eastern tropical South Pacific surface waters. *Proceedings of the National Academy of Sciences*, *113*(16), 4398–4403. https://doi.org/10.1073/pnas.1515641113

Laglera, L. M., & van den Berg, C. M. (2009). Evidence for geochemical control of iron by humic substances in seawater. *Limnology and Oceanography*, *54*, 610–619. https://doi.org/10.4319/lo.2009.54.2.0610

Loescher, C. R., Großkopf, T., Desai, F. D., Gill, D., Schunck, H., Croot, P. L., et al. (2014). Facets of diazotrophy in the oxygen minimum zone waters off Peru. *The ISME Journal*, *8*(11), 2180–2192. https://doi.org/10.1038/ismej.2014.71

Loh, A. N., & Bauer, J. E. (2000). Distribution, partitioning and fluxes of dissolved and particulate organic C, N and P in the eastern North Pacific and Southern Oceans. *Deep Sea Research Part I: Oceanographic Research Papers*, *47*(12), 2287–2316.

Luo, Y., Doney, S., Anderson, L., Benavides, M., Berman-Frank, I., Bode, A., et al. (2012). Database of diazotrophs in global ocean: Abundance, biomass, and nitrogen fixation rates. *Earth System Science Data*, *4*(1).

Martin, J. H., Knauer, G. A., Karl, D. M., & Broenkow, W. W. (1987). VERTEX: carbon cycling in the northeast Pacific. *Deep Sea Research*, *34*(2), 267–285. https://doi.org/10.1016/0198-0149(87)90086-0

Martinez-Perez, C., Mohr, W., Löscher, C. R., Dekaezemacker, J., Littmann, S., Yilmaz, P., et al. (2016). The small unicellular diazotrophic symbiont, UCYN-A, is a key player in the marine nitrogen cycle. *Nature Microbiology*, *1*(11), 16163. http://doi.org/10.1038/NMICROBIOL.2016.163

McGlathery, K. J., Risgaard-Petersen, N., & Christensen, P. B. (1998). Temporal and spatial variation in nitrogen fixation activity in the eelgrass Zostera marina rhizosphere. *Marine Ecology Progress Series*, *168*, 245–258. https://doi.org/10.3354/meps168245

Mulholland, M., Bernhardt, P., Ozmon, I., Procise, L., Garrett, M., O'Neil, J., et al. (2014). Contribution ofdiazotrophy to nitrogen inputs supporting Karenia brevis blooms in the Gulf of Mexico. *Harmful Algae*, *38*, 20–29. https://doi.org/10.1016/j.hal.2014.04.004

Mohr, W., Grosskopf, T., Wallace, D. W., & LaRoche, J. (2010). Methodological underestimation of oceanic nitrogen fixation rates. *PLoS ONE*, *5*(9), e12583. http://doi.org/10.1371/journal.pone.0012583

Moisander, P. H., Beinart, R. A., Hewson, I., White, A. E., Johnson, K. S., Carlson, C. A., et al. (2010). Unicellular cyanobacterial distributions broaden the oceanic N_2 fixation domain. *Science*, *327*(5972), 1512–1514. https://doi.org/10.1126/science.1185468

Moisander, P. H., Benavides, M., Bonnet, S., Berman-Frank, I., White, A. E., & Riemann, L. (2017). Chasing after non-cyanobacterial nitrogen fixation in marine pelagic environments. *Frontiers in Microbiology*, *8*, 1736. http://doi.org/10.3389/fmicb.2017.0173

Monteiro, F., Dutkiewicz, S., & Follows, M. (2011). Biogeographical controls on the marine nitrogen fixers. *Global Biogeochemical Cycles*, *25*, GB2003. http://doi.org/10.1029/2010GB003902

Montoya, J. P., Voss, M., Kahler, P., & Capone, D. G. (1996). A simple, high-precision, high-sensitivity tracer assay for N_2 fixation. *Applied and Environmental Microbiology*, *62*(3), 986–993.

Mulholland, M., Bernhardt, P., Widner, B., Selden, C., Chappell, P. D., Clayton, S., et al. (2019). High rates of N_2 fixation in temperate, western North Atlantic coastal waters expands the realm of marine diazotrophy. *Global Biogeochemical Cycles*, *33*, 826–840. https://doi.org/10.1029/2018GB006130

Mulholland, M. R., Bernhardt, P., Blanco-Garcia, J., Mannino, A., Hyde, K., Mondragon, E., et al. (2012). Rates of dinitrogen fixation and the abundance of diazotrophs in North American coastal waters between Cape Hatteras and Georges Bank. *Limnology and Oceanography*, *57*(4), 1067–1083. https://doi.org/10.4319/lo.2012.57.4.1067

Mulholland, M. R., Bronk, D. A., & Capone, D. G. (2004). Dinitrogen fixation and release of ammonium and dissolved organic nitrogen by Trichodesmium IMS101. *Aquatic Microbial Ecology*, *37*(1), 85–94. https://doi.org/10.3354/ame037085

Mulholland, M. R., Ohki, K., & Capone, D. G. (2001). Nutrient controls on nitrogen uptake and metabolism by natural populations and cultures of *Trichodesmium* (Cyanobacteria). *Journal of Phycology*, *37*(6), 1001–1009. https://doi.org/10.1046/j.1529-8817.2001.00080.x

Nedwell, D. B. (1999). Effect of low temperature on microbial growth: Lowered affinity for substrates limits growth at low temperature. *FEMS Microbiology Ecology*, *30*(2), 101–111. https://doi.org/10.1111/j.1574-6941.1999.tb00639.x

Parsons, T. R., Maita, Y., & Lalli, C. M. (1984). *A manual of biological and chemical methods for seawater analysis*. Oxford, UK: Publ. Pergamon Press.
Paulmier, A., & Ruiz-Pino, D. (2008). Oxygen minimum zones (OMZs) in the modern ocean. *Progress in Oceanography*, *80*(3-4), 113–128. https://doi.org/10.1016/j.pocean.2008.08.001
Postgate, J. (1998). *Nitrogen Fixation* (3rd Ed.). UK: Cambridge University Press.
Price, P. B., & Sowers, T. (2004). Temperature dependence of metabolic rates for microbial growth, maintenance, and survival. *Proceedings of the National Academy of Sciences*, *101*(13), 4631–4636. https://doi.org/10.1073/pnas.0400522101
Rahav, E., Bar-Zeev, E., Ohayion, S., Elifantz, H., Belkin, N., Herut, B., et al. (2013). Dinitrogen fixation in aphotic oxygenated marine environments. *Frontiers in Microbiology*, *4*, 227. http://doi.org/10.3389/fmicb.2013.00227
Rahav, E., Herut, B., Mulholland, M. R., Belkin, N., Elifantz, H., & Berman-Frank, I. (2015). Heterotrophic and autotrophic contribution to dinitrogen fixation in the Gulf of Aqaba. *Marine Ecology Progress Series*, *522*, 67–77. https://doi.org/10.3354/meps11143
Rees, A. P., Gilbert, J. A., & Kelly-Gerreyn, B. A. (2009). Nitrogen fixation in the western English Channel (NE Atlantic ocean). *Marine Ecology Progress Series*, *374*, 7–12. https://doi.org/10.3354/meps07771
Ripp, J. (1996). *Analytical detection limit guidance & laboratory guide for determining method detection limits*. PUBL-TS-056-96. Wisconsin Department of Natural Resources, Laboratory Certification Program.
Rue, E. L., & Bruland, K. W. (1995). Complexation of iron (III) by natural organic ligands in the Central North Pacific as determined by a new competitive ligand equilibration/adsorptive cathodic stripping voltammetric method. *Marine Chemistry*, *50*, 117–138.
Sakamoto, C. M., Friederich, G. E., & Codispoti, L. A. (1990). MBARI procedures for automated nutrient analyses using a modified Alpkem Series 300 Rapid Flow Analyzer. *Technical Report No. 90-2*. Monterey Bay, CA: Monterey Bay Aquarium Research Institute.
Severin, I., Bentzon-Tilia, M., Moisander, P. H., & Riemann, L. (2015). Nitrogenase expression in estuarine bacterioplankton influenced by organic carbon and availability of oxygen. *FEMS Microbiology Letters*, *362*(14). http://doi.org/10.1093/femsle/fnv105
Sharp, Z. (2017). *Principles of stable isotope geochemistry* (2nd ed.). https://digitalrepository.unm.edu/unm_oer/1/ (2 February 2019, date last accessed).
Shiozaki, T., Nagata, T., Ijichi, M., & Furuya, K. (2015). Nitrogen fixation and the diazotroph community in the temperate coastal region of the northwestern North Pacific. *Biogeosciences*, *12*(15), 4751–4764. http://doi.org/10.5194/bg-12-4751-2015
Sipler, R. E., Gong, D., Baer, S. E., Sanderson, M. P., Roberts, Q. N., Mulholland, M. R., & Bronk, D. A. (2017). Preliminary estimates of the contribution of Arctic nitrogen fixation to the global nitrogen budget. *Limnology and Oceanography Letters*, *2*(5), 159–166. https://doi.org/10.1002/lol2.10046
Sohm, J. A., Hilton, J. A., Noble, A. E., Zehr, J. P., Saito, M. A., & Webb, E. A. (2011). Nitrogen fixation in the South Atlantic Gyre and the Benguela upwelling system. *Geophysical Research Letters*, *38*, L16608. http://doi.org/10.1029/2011GL048315
Subramaniam, A., Yager, P., Carpenter, E., Mahaffey, C., Björkman, K., Cooley, S., et al. (2008). Amazon River enhances diazotrophy and carbon sequestration in the tropical North Atlantic Ocean. *Proceedings of the National Academy of Sciences*, *105*(30), 10,460–10,465. https://doi.org/10.1073/pnas.0710279105
Tang, W., Wang, S., Fonseca-Batista, D., Dehairs, F., Gifford, S., Gonzalez, A. G., et al. (2019). Revisiting the distribution of oceanic N_2 fixation and estimating diazotrophic contribution to marine production. *Nature Communications*, *10*(1), 831. https://doi.org/10.1038/s41467-019-08640-0
Thamdrup, B., Dalsgaard, T., & Revsbech, N. P. (2012). Widespread functional anoxia in the oxygen minimum zone of the Eastern South Pacific. *Deep Sea Research, Part I*, *65*, 36–45. https://doi.org/10.1016/j.dsr.2012.03.001
Tyrrell, T., & Law, C. (1997). Low nitrate:phosphate ratios in the global ocean. *Nature*, *387*(6635), 793–796. https://doi.org/10.1038/42915
van den Berg, C. M. (1995). Evidence for organic complexation of iron in seawater. *Marine Chemistry*, *50*, 139–157.
Vitousek, P. M., Cassman, K., Cleveland, C., Crews, T., Field, C. B., Grimm, N. B., et al. (2002). Towards an ecological understanding of biological nitrogen fixation. In E. W. Boyer, & R. W. Howarth (Eds.), *The nitrogen cycle at regional to global scales* (pp. 1–45). Dordrect: Springer. https://doi.org/10.1007/978-94-017-3405-9_1
Voss, M., Dippner, J. W., & Montoya, J. P. (2001). Nitrogen isotope patterns in the oxygen-deficient waters of the Eastern Tropical North Pacific Ocean. *Deep Sea Research Part I: Oceanographic Research Papers*, *48*(8), 1905–1921.
Weber, T., & Deutsch, C. (2014). Local versus basin-scale limitation of marine nitrogen fixation. *Proceedings of the National Academy of Sciences*, *111*(24), 8741–8746.
Welschmeyer, N. A. (1994). Fluorometric analysis of chlorophyll a in the presence of chlorophyll b and pheopigments. *Limnology and Oceanography*, *39*(8), 1985–1992. https://doi.org/10.4319/lo.1994.39.8.1985
Wen, Z., Lin, W., Shen, R., Hong, H., Kao, S.-J., & Shi, D. (2017). Nitrogen fixation in two coastal upwelling regions of the Taiwan Strait. *Scientific Reports*, *7*(1), 17601. http://doi.org/10.1038/s41598-017-18006-5
White, A. E., Foster, R. A., Benitez-Nelson, C. R., Masqué, P., Verdeny, E., Popp, B. N., et al. (2013). Nitrogen fixation in the Gulf of California and the Eastern Tropical North Pacific. *Progress in Oceanography*, *109*, 1–17. https://doi.org/10.1016/j.pocean.2012.09.002